Three-body calculation of πd elastic scattering observables at energies up to the (3,3) resonance

N. Giraud, Y. Avishai,* C. Fayard, and G. H. Lamot

Institut de Physique Nucléaire, Université Claude Bernard Lyon-I and IN2P3, 43 Bd du 11 Novembre 1918, 69621 Villeurbanne, France

(Received 20 June 1978)

The πd elastic scattering observables are calculated in the energy range 25 to 180 MeV on the basis of the Faddeev-Lovelace equations where relativistic kinematics are used only for the pion. In the (3,3) resonance region, the importance of all S, P πN channels (included in an exact way) and the sensitivity to the description of the deuteron wave function are demonstrated. The vector and tensor polarizations are predicted at 142 and 180 MeV.

[NUCLEAR REACTIONS πd elastic scattering, T_π=25–180 MeV, $d\sigma/d\Omega$, total cross section, vector and tensor polarizations, Faddeev calculation.]

I. INTRODUCTION

The pion-deuteron (πd) scattering problem seems to be of fundamental importance to nuclear physics, and it has gained an ever increasing amount of interest. On the one hand it contains most of the phenomena which are found in pion-nucleus (πA) scattering, while on the other hand it is closely related to the elementary processes of pion-nucleon (πN) and nucleon-nucleon (NN) scattering.

The rising interest in this problem resulted in a considerable progress in the experimental and the theoretical fronts as well. On the experimental side we are now able to get good quality elastic scattering data at various pion laboratory kinetic energies (T_π), while the first experiment on deuteron polarization is due in the near future. On the theoretical side, the progress is impressing just as well. The fact that the quantum mechanical three-body problem can be solved exactly is of extreme importance when applied to the πd system, since it provides the most reliable test for any approximation which is to be used in πA scattering problems. These include the single scattering approximation (SSA), the form factor approximation (FFA) (which are much in use at low energy due to the small πN cross section), as well as πA optical model and other approximations.

The solution of the three-body problem came with the use of Faddeev equations, but it took some time before reliable numerical results came out, in particular through the use of separable interactions. A rather extensive application of this formalism to the πd system has been carried out by Afnan and Thomas,[1] and Thomas.[2] It is now clear that while fully relativistic theories of πd reactions are in their first phase,[3,4] the nonrelativistic theory is well under control, and the amount of success is strongly related to the question of whether one has a reliable numerical code.

Yet, a careful examination of theoretical calculations of πd induced reactions provides a strong motivation for further investigations. To begin with, we feel that in view of the extreme complex nature of the calculations, there must be an independent check of Thomas results. But there are other points that should be examined carefully, namely the following:

(i) Most of the calculations performed so far assume that the πN interaction at medium energies ($120 < T_\pi < 250$ MeV) is dominated by the $\Delta(1236)$ resonance. (We shall term this assumption as the $P33$ scheme.) The obvious question is whether the inclusion of other πN partial waves, in particular all S and P partial waves is important, and to what extent. (The solution of the πd problem in which all S and P πN partial waves are retained in an exact manner is hereafter referred to as the SP scheme.)

(ii) In practically all previous calculations the coupling of two πd channels with l, $l' = J \pm 1$ orbital angular momenta has been neglected. (This coupling will be referred to as l, l' coupling.) Again, the question arises whether this neglect is justified.

(iii) The sensitivity of the results to the two nucleon (NN) interaction parameters has not been completely studied. In particular one would like to check the results for various values of the D-state probability in the deuteron wave function (P_D), in the SP scheme. Another interesting question is how the results are affected by using different parametrizations of the NN separable interactions such as Yamaguchi and Pieper-Reid. Besides, one must check whether NN rescattering effects in nondeuteron states (such as P or $^1S_0$) are important.

(iv) What are the predictions of the theoretical calculations for deuteron polarization observables?

These questions and many others provided the motivation for the present work. Partial answers to these questions have been given recently by ourselves.[5-7] In short, we have found that both the SP scheme and the l, l' coupling are of great importance in both cross section and polarization calculations, even at $T_\pi = 142$ MeV, which seems to be well covered by the P_{33} resonance.

In this paper we elaborate on the questions raised above, and provide reliable numerical results for various quantities at various energies. So far, the present calculations seem to be the most complete ones in the sense that points (i)–(iii) above are taken into account in an exact way, in combination with the use of relativistic kinematics for the pion.

The paper is organized as follows: In Sec. II the calculation scheme is described. It starts with the discussion of the three-body equations with relativistic pion kinematics (RPK). The relation between partial wave on-shell πd amplitudes $X^J_{l,l'}(E)$ and scattering observables is briefly studied, and then we move on to list the πN and NN two-body forces that will be used subsequently. Section III consists of our results, and is therefore the heart of the whole paper. The low energy domain, defined by $25 < T_\pi < 60$ MeV, is covered in Sec. III A, while the vicinity of the (3, 3) resonance is discussed in Sec. III B. Our results for total cross sections (elastic, inelastic, and total) are presented in Sec. III C while Sec. III D is devoted to polarization observables.

Few words about the presentation of the results in Sec. III are in order. The extreme complexity of the calculations combined with our limited knowledge of the reaction mechanism leave little room for careful interpretation of any single result. Thus, we feel that any attempt to draw definite conclusions is too ambitious, and therefore, the presentation of the results in Sec. III is done with the stress put on information rather than on interpretation.

Finally, we conclude the paper in Sec. IV in which some comparison with the fully relativistic (FR) results of Rinat and Thomas[3] is done. We also mention two directions for further investigations. In the low energy domain, the coupling to the absorption channel must be considered,[8,9] whereas at higher energies, inelastic effects in the πN system might be important especially in the explanation of the dip in the cross section at $\theta_{c.m.}$ around 150°.

II. THREE-BODY EQUATIONS AND TWO-BODY INPUT

This section describes the semirelativistic three-body equations and the separable NN and πN interactions used in the calculations.

A. Three-body equations

In the semirelativistic (SR) equations the nucleons are considered as nonrelativistic particles and relativistic kinematics are used only for the pion. This approximation is fully justified in the low energy range, and seems also reasonable in the resonance region (at $T_\pi = 142$ MeV, we have $v_N/c \sim 0.1$).

The SR equations can be derived in two ways. The first method proposed by Thomas[2] is based on the nonrelativistic Faddeev-Lovelace equations, modified by using relativistic pion kinetic energy (the corresponding equations are denoted hereafter RPK). In the second approach, we approximate the FR equations at first order in terms of the nucleon kinetic energy, and we thus get RPK2 equations which are very close to the RPK equations. This approach is more satisfactory but more tedious than the first one, and will not be described here. In Ref. 5, the complete derivation of the RPK2 equations is given, and it is also shown that the RPK equations can be deduced from RPK2 with only a few additional approximations. In what follows, we recall the main features in deriving the RPK equations, and we indicate what change occurs in RPK2.

Let us consider the πd system as a three-body system with two identical nucleons and the pion as third particle. The particles are interacting

TABLE I. Summary of the parametrizations used for the $^3S_1$–$^3D_1$ NN channels and for the S, P πN channels.

	N–N tensor forces			π–N forces		
Title	P_D	Reference	Notation	Partial waves	Reference	Notation
Yamaguchi	0%	11	Y0	all S and P	2	SP
	4%		Y4			
	7%		Y7			
Pieper rank 1	6.49%	12	P1	P_{33} alone	2	$P33$
Pieper rank 2	6.45%		P2			

pairwise through separable forces. The corresponding nonrelativistic Faddeev-Lovelace equations with inclusion of antisymmetrization coming from the identical nucleons have been given in explicit form by Afnan and Thomas.[1] Similar equations have been used by two of us in three-body calculations of $d\alpha$ elastic scattering.[10] In operator form, the equations read

$$X_{nm}=\sum_{\alpha} Z_{n\alpha}R_{\alpha}X_{\alpha m},$$
$$X_{\alpha m}=Z_{\alpha m}+\sum_{\beta} Z_{\alpha\beta}R_{\beta}X_{\beta m}+\sum_{n}Z_{\alpha n}R_{n}X_{nm}\,. \tag{1}$$

The n, m (α, β) labels refer to NN ($N\pi$) pairs. The Born terms $Z_{n\alpha}(Z_{\alpha\beta})$ correspond to the exchange of a pion (nucleon), and R_n (R_α) are the propagators of the NN ($N\pi$) pairs in the three-body Hilbert space. The physical elastic scattering amplitudes for $\pi+d\to\pi+d$ will be given by $2X_{dd}$ evaluated on the energy shell.

The equations (1) are then written in three-body Hilbert space, and, after angular momentum reduction, they are reduced to a set of coupled one-dimensional integral equations. The explicit form of these equations and of the partial wave Born amplitudes are given in Eqs. (B4)–(B5) of Ref. 1 or in Eqs. (16)–(17) of Ref. 10.

In the RPK approach proposed by Thomas,[2] one considers relativistic kinematics only for the pion, i.e., the nonrelativistic kinetic energy $q_\pi^2/2m_\pi$ is replaced by the invariant $t_\pi=(q_\pi^2+m_\pi^2)^{1/2}-m_\pi$. Therefore, using our notations of Ref. 10, one must insert the following modifications:

(i) The NN propagator in presence of the pion is, in the classical kinematics, $R_n(E-q_\pi^2/2\mu_{\pi,NN})$, where E is the three-body c.m. energy and $\mu_{\pi,NN}^{-1}=m_\pi^{-1}+(2m_N)^{-1}$. In RPK, it becomes $R_n(E-t_\pi-q_\pi^2/4m_N)$.

(ii) The resolvent of the free Hamiltonian appearing in the partial wave Born amplitudes for exchange of particle k reads, in the classical kinematics, $(E-q_i^2/2m_i-q_j^2/2m_j-q_k^2/2m_k)^{-1}$, where $\vec{q}_k=\vec{q}_i+\vec{q}_j$ is the momentum of the exchanged particle, and i, j, k are the particle labels. In RPK, when the label refers to a pion, t_π is used for the corresponding kinetic energy.

It can be shown[5] that two additional modifications must be introduced in RPK2.

(iii) The πN propagator in presence of the nucleon is $R_\alpha(E-q_N^2/2\mu_{N,\pi N})$, where the reduced mass becomes $\mu_{N,\pi N}^{-1}=m_N^{-1}+(m_N+m_\pi+E)^{-1}$, instead of $\mu_{N,\pi N}^{-1}=m_N^{-1}+(m_N+m_\pi)^{-1}$ which holds in RPK.

(iv) The relative momenta of the interacting pairs are given by the usual expressions[10]:

$$\vec{p}_i=-\rho_i\vec{q}_i-\vec{q}_j\,,\quad \rho_i=m_j/(m_j+m_k)\,,$$
$$\vec{p}_j=\vec{q}_i+\rho_j\vec{q}_j\,,\quad \rho_j=m_i/(m_i+m_k)\,, \tag{2}$$

where $(q_\pi^2+m_\pi^2)^{1/2}$ is used for the pion mass (instead of m_π in RPK).

The scattering amplitudes are obtained by solving the system of coupled one-dimensional integral equations. The singularities of the kernel are avoided by using the method of contour rotation, and we solve the system exactly with the Padé approximant technique following the procedure described in Ref. 5. One can then construct the scattering matrix $M(\theta)$ in the channel spin representation:

$$\langle 1\nu'|M(\theta)|1\nu\rangle=\sum_{J\mu lml'm'} X^{J}_{l'l}(q',q;s)\langle l'm'1\nu'|J\mu\rangle\langle J\mu|lm1\nu\rangle Y_{l'm'}(\hat{q}')Y^{*}_{lm}(\hat{q})\,. \tag{3}$$

Here, the channel spin is 1 with initial and final projections ν and ν', $\vec{J}=\vec{l}+\vec{1}=\vec{l}'+\vec{1}$ is the total spin, $\vec{q}$ and $\vec{q}'$ are the initial and final c.m. momenta with relative angle θ, and $X^{J}_{l'l}(q',q;s)$ are the physical scattering amplitudes ($q'=q=k$ = on-shell c.m. momentum).

The elastic differential cross section $\sigma(\theta)$ is calculated by

$$\sigma(\theta)=\tfrac{1}{3}[4\pi^2\mu_{\pi d}(k)]^2\mathrm{Tr}[M(\theta)M^\dagger(\theta)] \tag{4}$$

where

$$\mu_{\pi d}^{-1}(k)=m_d^{-1}+(k^2+m_\pi^2)^{-1/2}$$

(m_d is the deuteron mass).

The analyzing powers T_{kq} ($\pi+\vec{d}\to\pi+d$) and the polarizations t_{kq} ($\pi+d\to\pi+\vec{d}$) are evaluated through the relations

$$T_{kq}=\mathrm{Tr}(M\tau_{kq}M^\dagger)/\mathrm{Tr}(MM^\dagger),$$
$$t_{kq}=\mathrm{Tr}(MM^\dagger\tau_{kq})/\mathrm{Tr}(MM^\dagger)\,, \tag{5}$$

where the τ_{kq} are the spherical tensor operators relative to the deuteron.

In the above relations, the Madison convention is used for evaluating $M(\theta)$. Therefore the following relation holds: $t_{kq}=(-1)^{k+q}T_{kq}$.

For the practical calculation, one needs all partial wave amplitudes $X^{J}_{ll'}$ up to l, $l'=l_{\max}$ and $J=J_{\max}=l_{\max}+1$, where $l_{\max}$, $J_{\max}$ are reasonable cutoffs ($l_{\max}=7$ is sufficient for energies up to

200 MeV). The scattering amplitudes are obtained by solving the system with Padé [3/3] for $J=0$ to 3, and taking the single scattering approximation (SSA) $X^{\rm SSA}_{dd}=\sum_\alpha Z_{d\alpha}R_\alpha Z_{\alpha d}$ for $J=4$ to 8.

B. Two-body interactions

We only draw up the list of the NN and πN separable interactions used in our calculations. All these interactions have been described elsewhere in the literature, and one can find in the hereafter quoted references their parameters and characteristics (a summary is also given in Refs. 2, 5).

1. Nucleon-nucleon interactions

We take into account the $^3S_1$-$^3D_1$ channel, and only in one case, the $^1S_0$ and all the P waves are also introduced.

(i) For the $^3S_1-{}^3D_1$ channel, we take either Yamaguchi or Pieper parametrizations. The one-term Yamaguchi potentials are chosen to give $E_D=2.224$ MeV, $a_t=5.40$ fm, $r_t=1.73$ fm, and $Q=0.282$ fm^2, with D-state probabilities (P_D) 0%, 4%, and 7%. The interactions with $P_D=4\%$ and 7% are those of Phillips,[11] and the parameters of the interaction with $P_D=0\%$ are $\beta=1.436$ fm^{-1} (range) and $\lambda=-210.663$ MeV fm^{-1} (strength). These three interactions are phase equivalent only at low energy and lead to a poor description of the phase shifts: $\delta(^3S_1)$ is always positive and agrees with experiment only at low energy (up to 60 MeV), $\delta(^3D_1)$ has the wrong sign, and the mixing parameter ϵ_1 is not reproduced.

The Pieper-Reid separable interactions[12] are constructed in order to have the same deuteron wave function as the Reid soft-core (RSC) potential. We have used only the rank-1 and rank-2 parametrizations. Their deuteron properties are given in Ref. 12. The rank-1 potential has $P_D=6.49\%$ and leads to a similar description of the phase shifts as the Yamaguchi potentials. The rank-2 parametrization ($P_D=6.45\%$) is better in the sense that it gives a negative δ $(^3D_1)$ in correct agreement with experiment.

The differences between the Pieper and Yamaguchi interactions are also apparent in the shape of the deuteron form factors. The Pieper potentials have the same deuteron form factors as RSC, namely the monopole form factor $G_0(q)$ shows the diffraction minimum at $q\sim4.4$ fm^{-1} and the dipole form factor $G_2(q)$ has a broad maximum at $q\sim2$ fm^{-1} (see Fig. 2.7 of Ref. 13), while the Yamaguchi interactions give a nodeless G_0 reflecting their smooth character and a G_2 similar to the RSC one (see Fig. 2.11 of Ref. 13).

(ii) In the $^1S_0$ channel, we use Yamaguchi potential whose parameters are calculated in order to give the singlet low energy parameters $a_s=-20.31$ fm and $r_s=2.7$ fm.

(iii) For the $^1P_1$, $^3P_0$, $^3P_1$, and $^3P_2$ channels, we take one-term parametrizations adjusted to fit the corresponding phase shifts. The parameters are given in Refs. 14.

2. Pion-nucleon interactions

We choose the same potentials as Thomas[2] in the S and P πN channels. The parameters are determined by fitting the phase shifts and the scattering length (or volume). The problem of choosing which data to fit is discussed in Ref. 2 where one can find the results of the parameters search for the best πN potentials.

Table I summarizes the two-body forces used throughout. In what follows, the name of the calculation will be specified by two labels: The first one denotes the NN parametrization and the second one refers to the πN channels which are taken into account.

III. RESULTS AND DISCUSSIONS

We now present our results obtained with the semirelativistic equations in the energy range 25 to 180 MeV. For the sake of clarity, there will be four subsections concerning respectively the low energy domain (A), the resonance region (B), the total cross section (C) and the polarization observables (D).

We must emphasize that our code has been checked by comparing with the RPK results of Thomas at 142 MeV, using the Y4-$P33$ interactions. The agreement is complete as described in Ref. 6.

A. The low energy domain

At present time, there is only one recent set of experimental data for π^+d scattering at 47.7 MeV by Axen *et al.*,[15] but other π^+d and π^-d experiments are now in progress at Saclay for 25 MeV $<T_\pi<60$ MeV.[16] In order to compare with experiment, we include the effects of the Coulomb interaction at first order, following the approximate method of Thomas.[2] The full scattering amplitude is written as

$$X_{\pi^\pm d}=X^S_{\pi d}\pm X^C_{\pi d}\ . \tag{6}$$

$X^S_{\pi d}$ is the pure strong interaction amplitude obtained by solving the three-body equations, and $X^C_{\pi d}$ is the pure Coulomb amplitude evaluated at first order in the form factor approximation.[17-19] Figure 1 displays the results obtained at 25, 47.7, and 60 MeV with the Y4-SP interactions. The strong interference between Coulomb and nuclear forces is clearly reflected throughout the angular

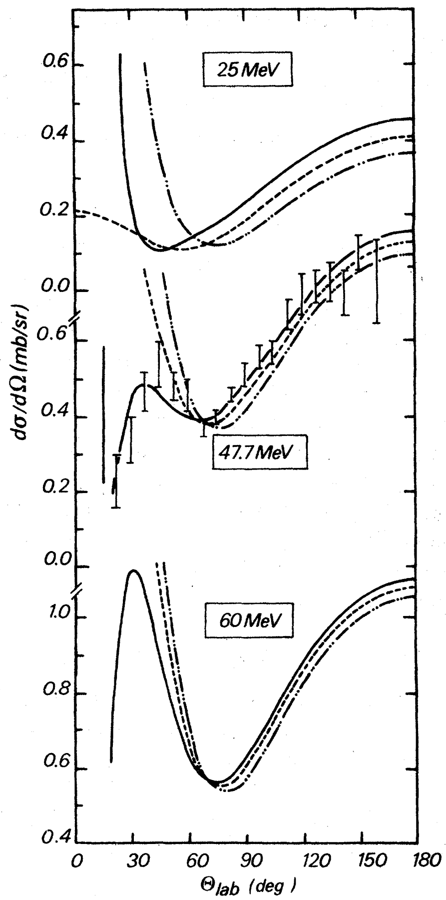

FIG. 1. Elastic differential cross sections at T_π =25.0, 47.7, and 60.0 MeV with the Y4-*SP* interactions. The Coulomb correction is added (——), subtracted (—··—··) or neglected (----). The experimental π^+d data at 47.7 MeV are from Ref. 15.

range, especially in the forward part. As shown in Fig. 2, the overall agreement with π^+d data at 47.7 MeV is good, the main discrepancies appearing in the region of the maximum near 40°. Changing the P_D value to 7% does not improve the situation. We notice that our results are very close to those of Thomas (see Fig. 8 of Ref. 2), the small changes reflecting the differences between the two calculations (Thomas neglects the l, l' coupling and some three-body channels are supposed to have a negligible effect). We also note that the behavior of the backward differential cross section with a change in P_D is different from that found in earlier calculations based on the single and double scattering approximation.[17-19]

We have tested the influence of the other *NN* channels by adding to the Y4-*SP* interaction the $^1S_0$ and all *P NN* partial waves. The effect at 47.7 MeV is rather small, the differential cross section being at most 2% higher than the Y4-*SP* curve. It

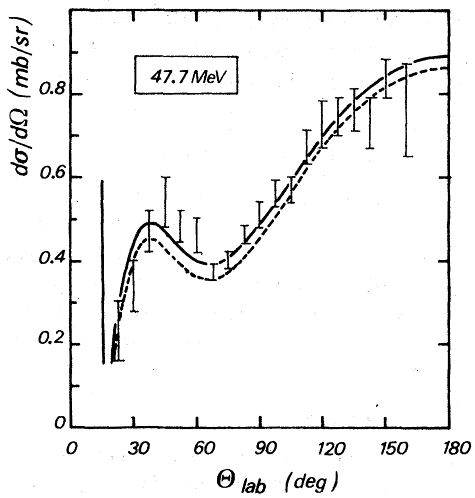

FIG. 2. Elastic differential cross sections at 47.7 MeV with the Y4-*SP* (——) and Y7-*SP* (----) interactions. The Coulomb correction is added, and the experimental π^+d data are from Ref. 15.

is thus justified to neglect the *NN* channels other than $^3S_1-{}^3D_1$.

B. The (3,3) resonance region

Most of the three-body calculations performed up till now in the $\Delta(3,3)$ resonance region use FR equations.[3,4] The study of Rinat and Thomas[3] seems to be the most complete in the sense that the importance of various truly relativistic effects and the influence of the *D*-state probability are investigated. However, some fundamental aspects are discarded in their calculations, namely (i) the l, l' coupling is neglected, (ii) only the $^3S_1-{}^3D_1$ *NN* and the P_{33} πN channels are taken into account, and (iii) the description of the tensor force is rather poor.

These approximations can be removed, but we are faced with the problem of solving systems of coupled integral equations of large order. The technique of Padé approximant makes possible the exact solution of such systems. Nevertheless, the computing time would be very large in the FR approach, and it seems reasonable in a first step to limit ourselves to the semirelativistic approach.

1. Effect of coupling and importance of relativistic effects

These two points have been discussed in Ref. 6 at T_π =142 MeV, and we only recall our conclusions:

(i) The effect of l, l' coupling is not negligible. Considering the scattering amplitudes $T^J_{ll'}$, the diagonal terms ($l=l'=J\pm1$) calculated with coupling are very close to those obtained without coupling, and the nondiagonal terms $T^J_{J-1,J+1}=T^J_{J+1,J-1}$ are of the same order of magnitude as $T^J_{J+1,J+1}$. The Y4-*P*33 differential cross section calculated with coupling is identical to that calculated without coupling in the forward part, but becomes up to 7% higher at backward angles. This effect on the cross section is not essential, but we will show in Sec. III D that the tensor polarizations are very sensitive to the coupling.

(ii) The importance of relativistic effects was investigated by comparing the RPK and RPK2 results obtained at 142 MeV with the Y4-*P*33 and Y4-*SP* interactions. The results given in Table I of Ref. 6 show clearly that a more correct treatment of the relativistic effects by means of RPK2 produces a significant decrease mainly in the backward differential cross section, and that the relativistic effects become smaller in the *SP* scheme than in the *P*33 scheme. (In the *P*33 scheme, the differential cross section at 180° is lower by about 11% in RPK 2 than in RPK, and in the *SP* scheme this difference is about 6%.)

In what follows, all the results have been obtained in RPK theory with l, l' coupling included.

2. The SP and P33 schemes

In order to study the effect of introducing the other S, P πN channels in addition to P_{33}, we compare the results obtained in the *P*33 and *SP* schemes with the same tensor force. The calculations have been performed at 142 and 180 MeV with the Y4 and P2 parametrizations.

In Fig. 3(a), we give the Y4-*P*33 and Y4-*SP* curves at 142 MeV. The effect of the *SP* scheme is to lower strongly the differential cross section throughout the angular range (the decrease is 26% at 0°, 12% at 90°, and 40% at 180°). Referring to the experimental data, the improvement of Y4-*SP* calculation in comparison with Y4-*P*33 is obvious, even if the backward region remains too high.

The P2-*P*33 and P2-*SP* results at 142 MeV are shown in Fig. 3(b). As in the Y4 calculation, the *SP* scheme improves the agreement with experiment. However, we note that the backward decrease is smaller in the P2 calculation (20% at 180°) than in Y4.

Similar trends appear at 180 MeV as shown in Fig. 4(a) and 4(b). The agreement with experiment throughout the angular range is better when all S, P πN channels are included, and we note that the decrease at forward angles is smaller (~9% at 0°) than at 142 MeV.

We can now conclude the following:

(i) The inclusion (in an exact way) of all S and P πN channels brings very large effect in the RPK calculations, especially at backward angles, and improves systematically the agreement with experimental data.

(ii) Even at energy close to the (3,3) resonance where the P_{33} should dominate, the decrease of the cross section due to the *SP* scheme is important.

(iii) The effect at backward angles is strongly reduced when the *NN* tensor force is more realistic.

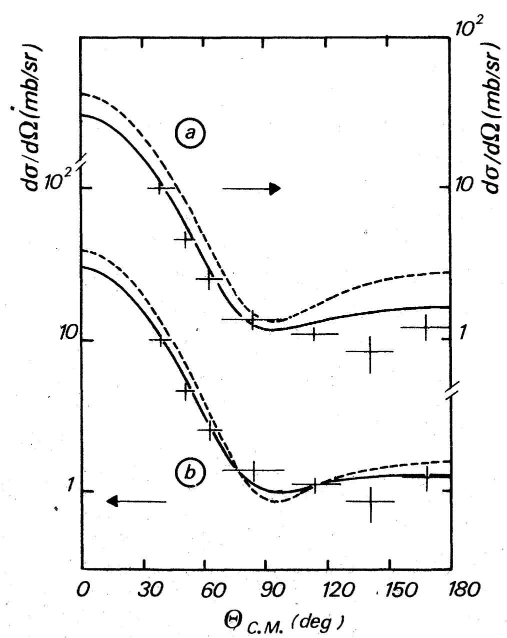

FIG. 3. Elastic differential cross section at T_π =142 MeV using the Y4 3(a) or P2 3(b) tensor forces, and the *SP* (——) or *P*33 (---) schemes. Experimental data are from Ref. 20.

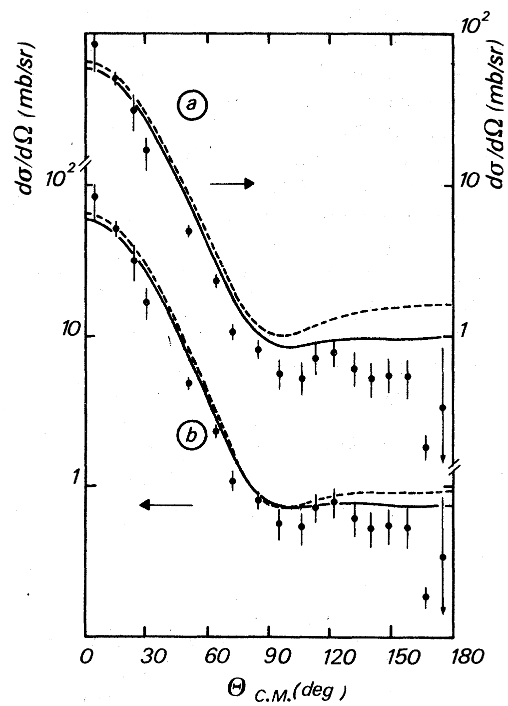

FIG. 4. Same as Fig. 3 for T_π =180 MeV. Experimental data are from Ref. 21.

In Ref. 5, we have evaluated the differential cross section at 142 MeV using the single scattering approximation. The calculation has been done with the Y4 tensor force in the *SP* and *P*33 schemes. We found that the decrease due to the *SP* scheme is ~ 20% at forward angles, but is negligible in the backward domain. Comparing with the above results, we conclude that the perturbative treatment at lowest (second) order of all other than P_{33} πN channels is not sufficient here, and the large effect at backward angles appears only in the exact calculation.

3. Influence of the NN tensor force

Here, we investigate the sensitivity of the differential cross section to the description of the $^3S_1 - {}^3D_1$ *NN* channel.

First of all, we consider the effect of the *D*-state percentage value of the deuteron by using the Y0, Y4, and Y7 parametrizations. An increase of P_D from 0% to 7% lowers slightly the differential cross section throughout the angular range, as well in the Y-*P*33 as in the Y-*SP* calculations. The results obtained at 142 MeV are given in Table II, and similar conclusions hold at 180 MeV. This effect is small in comparison with the effect found by Rinat and Thomas[3] in the FR approach where the backward cross section is reduced up to 25% at 180° when P_D goes from 4% to 6.7%. However, one must remember that the one-term tensor forces used in our calculations and also in the FR approach do not give an equivalent description of the $^3S_1 - {}^3D_1$ channel when the P_D value is changed. It is therefore incorrect to set down the observed variations only to a genuine effect of P_D.

The results of Figs. 3 and 4 show clearly that the Pieper tensor force (P2) leads to a better agreement with experimental data than the Yamaguchi interaction, as well in the *P*33 as in the *SP* scheme. One must attribute this effect to the fact that the P2 potential gives a better description of the $^3S_1$-$^3D_1$ channel than Yamaguchi, namely as regards to the phase shifts and to the deuteron wave function. We also have calculated the differential cross-section at 142 MeV with the P1 interaction which has the same deuteron wave function as P2 and phase shifts similar to the Yamaguchi ones [namely $\delta(^3D_1)$ has the wrong sign]. The P1-*SP* results are found to be slightly higher than the P2-*SP* results throughout the angular range (the variation is at most ~3%). Therefore, the large differences (mainly at backward angles) between the Pieper and Yamaguchi results must be attributed to the difference in the description of the deuteron wave function rather than to the details of the *NN* phase shifts, and it appears essential to use a $^3S_1 - {}^3D_1$ parametrization which gives above all a realistic deuteron wave function.

4. Effect of the other NN channels

The role of the other *NN* channels in the resonance region has been tested by adding to the Y4-*SP* interaction the $^1S_0$ and all *P NN* partial waves. The effect at 142 MeV is comparable with that found in the low energy domain: The differential cross section is slightly higher than the Y4-*SP* curve, the variation being 4% in the minimum region and 2% at backward angles. Retaining the $^3S_1 - {}^3D_1$ *NN* channel only is therefore a good approximation in the resonance region.

C. Elastic, reaction, and total cross sections

The elastic cross section $\sigma_{el}(E)$ is obtained by integrating the differential cross sections $d\sigma/d\Omega$ at each energy E

$$\sigma_{el}(E) = \int d\Omega \, \frac{d\sigma}{d\Omega}(E) \, . \tag{7}$$

The reaction cross section $\sigma_R(E)$ is given by the usual relation

$$\sigma_R(E) = \frac{4\pi}{3k^2} \sum_{Jll'} (2J+1)(\delta_{ll'} \, \mathrm{Im} C^J_{l'l} - |C^J_{l'l}|^2) \, , \tag{8}$$

where the $C^J_{l'l}$ are expressed in terms of the on-shell scattering amplitudes as

$$C^J_{l'l} = -\pi \mu_{\pi d}(k) k X^J_{l'l} \, .$$

TABLE II. Sensitivity of the elastic differential cross section at 142 MeV to the *D*-state probability, in the *P*33 and *SP* schemes.

Calculation	Elastic differential cross section (in mb/sr) $\theta_{c.m.} = 0°$	$\theta_{c.m.} = 90°$	$\theta_{c.m.} = 180°$
Y0-*P*33	42.68	1.34	3.00
Y4-*P*33	42.15	1.32	2.71
Y7-*P*33	41.48	1.26	2.67
Y0-*SP*	30.79	1.15	1.68
Y4-*SP*	30.58	1.15	1.59
Y7-*SP*	29.96	1.09	1.60

At last, we calculate the total cross section $\sigma_T(E) = \sigma_{el}(E) + \sigma_R(E)$. These quantities have been evaluated in the energy range 25 to 256 MeV, with the Y4-*SP* interactions. In Fig. 5, we give the results and compare the total cross section with the recent experimental data obtained at the Swiss Institute for Nuclear Research (SIN)[22] (in fact, we have plotted the mean value of the π^+d and π^-d experimental total cross sections). The general trend is correctly reproduced, and the agreement is rather good in the resonance region.

At energies below the resonance, the theoretical results are lower than experiment. One can attribute the discrepancy to the lack of pion absorption in our model. Indeed, the reaction cross section we have calculated here is the $\pi + d \rightarrow \pi + N + N$ break-up cross section, the $\pi + d \rightarrow N + N$ absorption process being not included. We can simulate the effect of absorption by adding to our results the $\pi + d \rightarrow p + p$ experimental cross-section (see for example Spuller and Measday[23] for a summary of the existing data). For energies up to 250 MeV, this cross section varies between 4 and 10 mb (see Fig. 3 of Ref. 23), and clearly such a correction improves the agreement of our results with experiment for energies up to the resonance. At energies above the resonance, the correction due to absorption is rapidly decreasing with increasing energy, and the discrepancy between theory and experiment should arise mainly from the incomplete treatment of relativistic effects in the RPK approach, combined with the possibility of pion production.

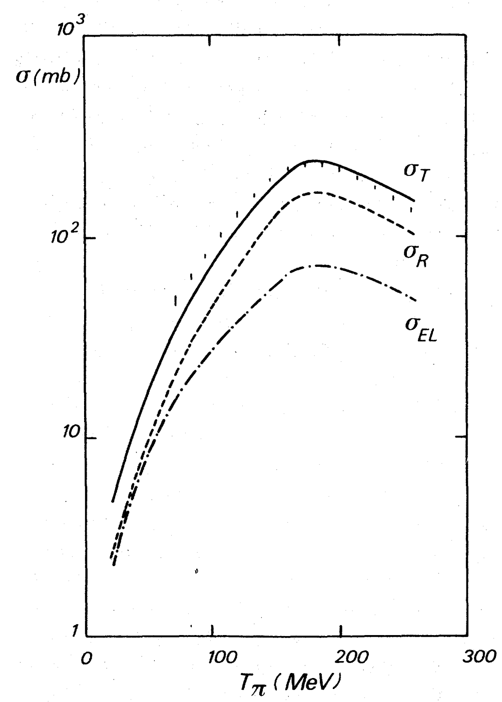

FIG. 5. Elastic (—·—·), reaction (---) and total cross sections (——) calculated with the Y4-*SP* interactions. The experimental results are the mean values of the π^+d and π^-d experimental cross sections given in Ref. 22.

D. Predictions for polarization parameters

Experiments that involve polarizations are hard to perform, but they can give valuable informations on the nature of the forces among the particles involved, especially their spin dependence. It is our belief that with the advent of meson factories, polarization experiments induced by πd elastic scattering will receive particular attention. The first experiment in this category proposed by Grüebler *et al.*[24] (and now in progress at SIN) concerns the determination of the tensor polarization t_{20} (the only tensor observable which is nonzero at 180°) in the $\pi + d \rightarrow \pi + \vec{d}$ scattering, and we think that now is the time to present some theoretical investigations.

Since we know the scattering amplitudes, the vector (it_{11}) and tensor (t_{20}, t_{21}, t_{22}) polarizations are easily calculated according to Eq. (5) of Sec. II. Here, we present our results at 142 and 180 MeV (part of them have been discussed in a previous letter[7]). We have investigated (i) the effect of the *SP* scheme, (ii) the importance of l, l' coupling, and (iii) the sensitivity to the description of the $^3S_1$-$^3D_1$ *NN* channel. We will discuss mainly the it_{11} and t_{20} observables. The quantity t_{20} (180°) at 142 MeV will receive particular attention since it will be the first available data.

The angular distribution of the vector polarization it_{11} at 142 MeV with the P2 – *P*33 and P2-*SP* interactions are shown in Fig. 6(a). The structure of it_{11} in the angular range 0° to 120° changes completely when all *S*, *P*, πN channels are included in addition to the P_{33}. Using any other tensor force like P1, Y0, Y4, or Y7, we found *P*33 and *SP* results close to the P2-*P*33 and P2-*SP* results, respectively. We have also noted that neglecting the l, l' coupling did not affect the results. Similar conclusions hold at 180 MeV, namely the effect of using all *S*, *P* πN channels and not the P_{33} alone is still very large as shown in Fig. 6(b).

In conclusion, the vector polarization it_{11} is rather insensitive to the description of the $^3S_1$-$^3D_1$ *NN* channel and its structure is highly dependent on the inclusion of all *S*, *P* πN channels. A conclusive experiment would be to measure it_{11} near $\theta_{c.m.} = 80°$ where the theoretical value is about 0.4 in the *SP* scheme and an order of magnitude lower in the *P*33 scheme.

We now come to the tensor polarizations. At first, we find that the *SP* scheme leads to nonnegligible effects on the *P*33 scheme, but, in

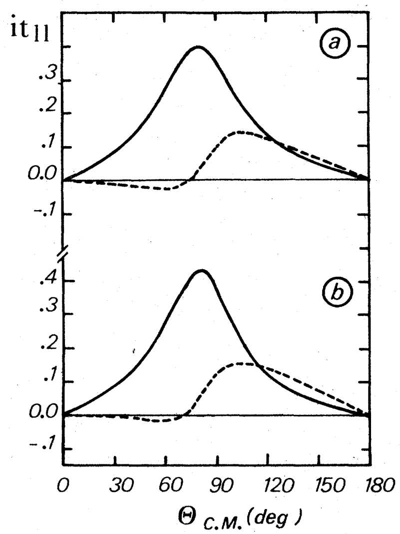

FIG. 6. Vector polarization it_{11} with the P2-SP(——) and P2-P33 (---) interactions at 142 MeV 6(a) and 180 MeV 6(b).

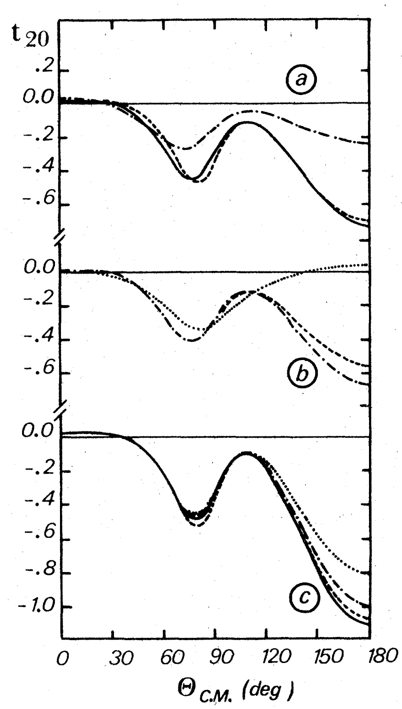

FIG. 7. Tensor polarization t_{20} at 142 MeV 7(a) and 7(b) and 180 MeV 7(c). In 7(a), the used interactions are P2-P33 (---), and P2-SP with coupling (——) and without coupling (—·—·). In 7(b), the sensitivity to the D-state percentage value is shown: The SP scheme is assumed, and the forces are Y0 (·····), Y4 (---), and Y7 (—·—·). In 7(c), the used interactions are P2-P33 (---), P2-SP (——), Y4-SP (·····), and Y7-SP (—·—·).

contrast with it_{11}, does not change the structure of the curves. This is illustrated in Fig. 7(a) for the quantity t_{20} calculated at 142 MeV with the P2 tensor force. We note a small variation of t_{20} (180°), the P2-SP value being ~4% lower than the P2-P33. A similar effect appeared when using the P1 tensor force, but the variation was found to be larger (~14%) in the calculations assuming the Y4 and Y7 tensor forces. Therefore, the effect of the SP scheme on t_{20} (180°) is strongly reduced when the NN tensor force is more realistic (a similar conclusion was drawn for the differential cross section in Sec. III B 2).

In the second step, we consider the importance of l, l' coupling. In Fig. 7(a), we report the P2-SP results for t_{20} without coupling. The effect in the angular range 30° to 180° is dramatic, and the same situation appears for t_{21} and t_{22}. One must therefore take into account the l, l' coupling in calculating tensor polarizations.

Next, we investigate the sensitivity to the description of the tensor force. We concentrate on t_{20} which is of interest for the near future. This quantity is sensitive to the D-state percentage value, especially at backward angles as shown in Fig. 7(b). For Yamaguchi tensor forces, t_{20} (180°) decreases with increasing P_D, its values for $P_D = 0\%$, 4%, and 7% being respectively 0.04, −0.56, and −0.67. On the other hand, from the comparison between the Y7-SP and P2-SP results corresponding to tensor forces which have similar D-state probabilities but different deuteron wave functions, we infer that the backward part of t_{20} is slightly model dependent [t_{20} (180°) takes the values −0.73 and −0.67 for the P2 and Y7 interactions, respectively]. Since the P1-SP and P2-SP results were found to be practically identical, this effect appears to be directly related to the description of the deuteron wave function, as it was the case for the differential cross section (Sec. III B 3). We note that the corresponding variations in t_{20} (180°) are smaller than the variations due to a change in P_D from 4% to 7%. Therefore, provided that the experimental accuracy will be good enough, there will be a chance to determine P_D by measuring t_{20} (180°) as proposed by Grüebler *et al.*[24]

An equivalent study of the tensor polarizations at 180 MeV shows that the above conclusions are still valid. As an example, we give in Fig. 7(c) the angular distributions of t_{20} calculated with the P2-P33, P2-SP, Y4-SP and Y7-SP interactions.

Let us compare our results with those based on other models. Our prediction for t_{20} at 142 MeV is in good agreement with that obtained by Gibbs[25] in a multiple scattering approach, namely the dependence of t_{20} (180°) as a function of P_D is similar. However, contrary to his statement,

it_{11} is by no means small as can be seen from Fig. 6(a). Our results for it_{11} at 142 and 180 MeV assuming the P_{33} dominance resemble in shape to those of Händel *et al.*[26] who used a D^* model for the πd scattering. However, the effect of the other S, P πN channels in addition to P_{33} should be investigated in this model.

At last, we point out that the relativistic effects on the polarization observables were found to be small when using the RPK2 equations. We have also noted that introducing the $^1S_0$ and P NN channels brings small change in the polarization parameters, the most noticeable variation being a 6% decrease in t_{20} (180°).

IV. CONCLUDING REMARKS

We have presented here extensive three-body calculations of πd elastic scattering observables. Within the pure three-body theory, most of the important aspects have been included in an exact manner, and the quality of the results obtained up to the resonance region is very encouraging for further theoretical and experimental work. In the resonance region two fundamental conclusions have been drawn from the RPK approach, namely (i) the effect of introducing in an exact way all the S, P πN channels is very important, and (ii) it is essential to use a parametrization of the $^3S_1$-$^3D_1$ NN channel giving a realistic deuteron wave function. At this point, it is worthwhile to locate the points of agreement as well as discrepancy with the FR results obtained by Rinat and Thomas[3] and by Rinat *et al.*[27] (concerning this recent preprint, we are only interested here in the results calculated without π absorption). Those points concern the effect of P_D on the cross section at backward angles, the l, l' coupling and the $P33$ versus the SP schemes.

As we pointed out in Sec. III B 3, we disagree with the results of Ref. 3 in the sense that changing P_D from 4% to 7% lowered $d\sigma/d\Omega$ (180°) by 3% in our calculations and by 25% in those of Ref. 3. It must be pointed out that calculations based on the SSA by McMillan and Landau[17] led to an increase of $d\sigma/d\Omega$ (180°) with increasing P_D. Except for the different origin of the two sets of equations, and the insufficient description of the deuteron by Yamaguchi form factors, we do not know the reason for this discrepancy.

In Ref. 27, FR calculations at 180 MeV are performed in which the πN partial waves other than the P_{33} are included in the SSA [Eq. (3) therein] and it is claimed that this is sufficient. We repeat here our claim in Sec. III B 2, that in our view, this is not enough. The effect of the SP scheme found by Rinat *et al.* on the differential cross section is apparent only in the backward hemisphere, especially in the calculation at $P_D = 6.7\%$, and, contrary to our results, the SP curve is found higher than the $P33$ curve.

The polarization observables calculated in Ref. 27 look similar to ours, and the same behavior appears as regards to the various effects, namely the change in it_{11} due to the SP scheme, the effect of l, l' coupling on tensor polarizations, and the sensitivity of t_{20} (180°) to the D-state percentage value.

It should be of great interest to complete the existing studies by performing fully relativistic calculations including in an exact way all S, P πN channels and using a realistic NN tensor force.

Finally, we shall mention two ways of further theoretical investigations. In the low energy domain, the absorption channel must be taken into account, in order to account for πd scattering length, as well as low energy cross sections and polarization observables. In the "high" energy region, inelastic production channels start to be important. The incorporation of these effects can be done in a straightforward manner by using the input obtained from the solution of the coupled channel πN equations suggested by Londergan, McVoy, and Moniz.[28] Such an attempt might be important in accounting for the dip in the cross section at $T_\pi = 256$ MeV, which so far remained unexplained.

ACKNOWLEDGMENT

We would like to thank A. S. Rinat and A. W. Thomas for very helpful remarks, and for sending us Ref. 27 prior to publication. Fruitful discussions with E. Elbaz during the course of the present work are highly appreciated.

*On leave of absence from Ben Gurion University, Beer-Sheva, Israel.
[1]I. R. Afnan and A. W. Thomas, Phys. Rev. C 10, 109 (1974).
[2]A. W. Thomas, Nucl. Phys. A258, 417 (1976).
[3]A. S. Rinat and A. W. Thomas, Nucl. Phys. A282, 365 (1977).
[4]R. M. Woloshyn, E. J. Moniz, and R. Aaron, Phys. Rev. C 13, 286 (1976); V. B. Mandelzweig, H. Garcilazo, and J. M. Eisenberg, Nucl. Phys. A256, 461 (1976); A264, 531 (1976); J. M. Riveira and H. Garcilazo, Nucl. Phys. A285, 505 (1977); D. D. Brayshaw and E. Ferreira, Phys. Lett. 68B, 139 (1977); T. J. Kopaleishvili, A. I. Machavariani, and G. A. Emelyanenko, Report No. E4-10943, 1977 (unpublished).
[5]N. Giraud, Thèse de Troisième Cycle, Université

Lyon-I, Report No. LYCEN 7805, 1978 (unpublished).
[6]N. Giraud, G. H. Lamot, and C. Fayard, Phys. Rev. Lett. 40, 438 (1978).
[7]N. Giraud, Y. Avishai, C. Fayard, and G. H. Lamot, Phys. Lett. 77B, 141 (1978).
[8]T. Mizutani and D. Koltun, Ann. Phys. (N.Y.) 109, 1 (1977).
[9]A.S. Rinat, Nucl. Phys. A287, 399 (1977).
[10]B. Charnomordic, C. Fayard, and G. H. Lamot, Phys. Rev. C 15, 864 (1977).
[11]A. C. Phillips, Nucl. Phys. A107, 209 (1968).
[12]S. C. Pieper, Phys. Rev. C 9, 883 (1973).
[13]J. S. Levinger, in *Springer Tracts in Modern Physics*, edited by G. Höhler (Springer, New York, 1974), Vol. 71, pp. 88–240.
[14]The parameters of the $^3P_0$ are from P. Doleschall, Nucl. Phys. A201, 264 (1974), and the parameters of the $^1P_1$, $^3P_1$, and $^3P_2$ are from W. Plessas, L. Mathelitsch, F. Pauss, and H. F. K. Zingl, Univ. of Graz report, 1976 (unpublished).
[15]D. Axen, G. Duesdieker, L. Felawka, G. Ingram, R. Johnson, G. Jones, D. Lepatourel, M. Salomon, W. Westlund, and L. Robertson, Nucl. Phys. A256, 387 (1976).
[16]B. Saghaï *et al.*, private communication.
[17]M. McMillan and R. H. Landau, TRIUMF Report No. TRI-74-1, 1974 (unpublished).
[18]H. N. Pendelton, Phys. Rev. 131, 1833 (1963).
[19]C. Carlson, Phys. Rev. C 2, 1224 (1970).
[20]E. G. Pewitt, T. H. Fields, G. B. Yodh, J. G. Fetkovich, and M. Derrick, Phys. Rev. 131, 1826 (1963).
[21]J. H. Norem, Nucl. Phys. B33, 512 (1971).
[22]E. Pedroni, K. Gabathuler, J. J. Domingo, W. Hirt, P. Schwaller, J. Arvieux, C. H. Q. Ingram, P. Gretillat, J. Piffaretti, N. W. Tanner, and C. Wilkin, SIN Report No. PR-77-004, 1977 (unpublished).
[23]J. Spuller and D. F. Measday, Phys. Rev. D 12, 3550 (1975).
[24]W. Grüebler *et al.*, SIN proposal R-73-01.1 (unpublished).
[25]W. R. Gibbs, Phys. Rev. C 3, 1127 (1971).
[26]R. Händel, M. Dillig, and M. G. Huber, Phys. Lett. 73B, 4 (1978).
[27]A. S. Rinat, E. Hammel, Y. Starkand, and A. W. Thomas, Report No. WIS-78/17-Ph (unpublished).
[28]J. T. Londergan, K. W. McVoy, and E. J. Moniz, Ann. Phys. (N.Y.) 86, 147 (1974).